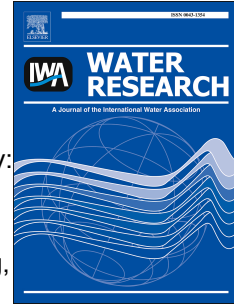


Journal Pre-proof



Synthesized trade-off analysis of flood control solutions under future deep uncertainty:
An application to the central business district of Shanghai

Hengzhi Hu, Zhan Tian, Laixiang Sun, Jiahong Wen, Zhuoran Liang, Guangtao Dong,
Junguo Liu

PII: S0043-1354(19)30841-3

DOI: <https://doi.org/10.1016/j.watres.2019.115067>

Reference: WR 115067

To appear in: *Water Research*

Received Date: 4 May 2019

Revised Date: 5 September 2019

Accepted Date: 6 September 2019

Please cite this article as: Hu, H., Tian, Z., Sun, L., Wen, J., Liang, Z., Dong, G., Liu, J., Synthesized trade-off analysis of flood control solutions under future deep uncertainty: An application to the central business district of Shanghai, *Water Research* (2019), doi: <https://doi.org/10.1016/j.watres.2019.115067>.

This is a PDF file of an article that has undergone enhancements after acceptance, such as the addition of a cover page and metadata, and formatting for readability, but it is not yet the definitive version of record. This version will undergo additional copyediting, typesetting and review before it is published in its final form, but we are providing this version to give early visibility of the article. Please note that, during the production process, errors may be discovered which could affect the content, and all legal disclaimers that apply to the journal pertain.

© 2019 Published by Elsevier Ltd.

1 **Synthesized trade-off analysis of flood control solutions under future deep**
2 **uncertainty: An application to the central business district of Shanghai**

3
4 Hengzhi Hu^{1, †}, Zhan Tian^{2, †}, Laixiang Sun^{3,4,5,*}, Jiahong Wen^{1,*}, Zhuoran Liang⁶, Guangtao
5 Dong⁷, Junguo Liu²

6
7 ¹ Department of Environmental and Geographical Sciences, Shanghai Normal University,
8 Shanghai 200234, China

9 ² School of Environmental Science and Engineering, Southern University of Science and
10 Technology, Shenzhen 518055, China

11 ³ Department of Geographical Sciences, University of Maryland, College Park, MD 20742,
12 USA

13 ⁴ School of Finance and Management, SOAS University of London, London WC1H 0XG,
14 UK

15 ⁵ International Institute for Applied Systems Analysis (IIASA), A-2361 Laxenburg, Austria

16 ⁶ Hangzhou Meteorological Services, Hangzhou, Zhejiang, China

17 ⁷ Shanghai Climate Center, Shanghai Meteorological Service, Shanghai 200030, China

18

19 [†] Hengzhi Hu and Zhan Tian contribute equally to this article.

20 * Correspondence: lsun123@umd.edu (L.S.); jhwen@shnu.edu.cn (J.W.)

21 **Synthesized trade-off analysis of flood control solutions under future deep**
22 **uncertainty: An application to the central business district of Shanghai**

23

24 **Abstract**

25 Coastal mega-cities will face increasing flood risk under the current protection standard
26 because of future climate change. Previous studies seldom evaluate the comparative
27 effectiveness of alternative options in reducing flood risk under the uncertainty of future
28 extreme rainfall. Long-term planning to manage flood risk is further challenged by
29 uncertainty in socioeconomic factors and contested stakeholder priorities. In this study, we
30 conducted a knowledge co-creation process together with infrastructure experts, policy
31 makers, and other stakeholders to develop an integrated framework for flexible testing of
32 multiple flood-risk mitigation strategies under the condition of deep uncertainties. We
33 implemented this framework to the reoccurrence scenarios in the 2050s of a record-breaking
34 extreme rainfall event in central Shanghai. Three uncertain factors, including precipitation,
35 urban rain island effect and the decrease of urban drainage capacity caused by land
36 subsidence and sea level rise, are selected to build future extreme inundation scenarios in the
37 case study. The risk-reduction performance and cost-effectiveness of all possible solutions are
38 examined across different scenarios. The results show that drainage capacity decrease caused
39 by sea-level rise and land subsidence will contribute the most to the rise of future inundation
40 risk in central Shanghai. The combination of increased green area, improved drainage system,
41 and the deep tunnel with a runoff absorbing capacity of 30% comes out to be the most
42 favorable and robust solution which can reduce the future inundation risk by 85% ($\pm 8\%$).
43 This research indicates that to conduct a successful synthesized trade-off analysis of
44 alternative flood control solutions under future deep uncertainty is bound to be a knowledge
45 co-creation process of scientists, decision makers, field experts, and other stakeholders.

46

47 **Keyword:** Decision-making under deep uncertainty; urban flood solutions; cost-effectiveness;
48 climate change; China.

49

50 **Introduction**

51 Climate change presents a significant planning challenge for mega-cities. With a
52 population greater than 10 million, mega-cities are typically the most prominent population
53 and economic centers of their home countries (United Nations, 2018). Observational
54 evidence over the 20th and early 21st century shows that the globally averaged rate of increase
55 in annual maximum daily rainfall intensity was between 5.9% and 7.7% per °C of globally
56 averaged near-surface atmospheric temperature (Westra et al., 2013, 2014). In addition to this
57 global trend, increased urbanization, which is associated with anthropogenic heat and
58 artificial land cover, may lead to an effect of urban rain island in a localized heavy rainfall
59 event. The urban rain island effect means that the center of the city receives much more
60 precipitation than the surrounding suburbs. Such an effect has been observed in Tokyo, Japan
61 (Souma et al, 2013; Shimoju et al, 2010; Kusaka et al, 2014), Mumbai, India (Paul et al.
62 2018), and Shanghai, China (Gu et al., 2015; Liang and Ding, 2017). Looking to the next few
63 decades, it is expected with high confidence that the intensity and/or frequency of extreme
64 daily rainfall will continue to increase, especially in urban areas (IPCC, 2014; Kharin et al.,
65 2007; Westra et al., 2014; Wu et al. 2013).

66 Mega-cities are therefore positioned to play a leading role in responding to climate
67 change challenges and are in need of knowledge to aid in their planning efforts under deep
68 uncertainty (Aerts et al., 2013, 2014; Rosenzweig et al., 2011). Given the fact that
69 rainfall-derived floods have been one of the most costly and dangerous natural hazards
70 worldwide (Hallegatte et al., 2013; CRED, 2014), it is of great socioeconomic significance to

71 improve our understanding of the changing behavior and impacts of extreme rainfall (Westra
72 et al., 2014) and to find robust solutions for the planning and design of flood protection
73 infrastructures (Löwe et al., 2017). There is a large body of literature assessing the inundation
74 risk under future extreme precipitation scenarios (e.g., among others, Huong and Pathirana,
75 2013; Jenkins et al., 2017; Muis et al., 2015; Poelmans et al., 2011; Sekovski et al., 2015;
76 Teng et al., 2017; Wu et al., 2018). However, as pointed out by Löwe et al. (2017), such
77 scenario-based evaluations are difficult to apply for planning and design purposes owing to
78 their heavy simulation loads and are therefore typically performed only for a few selected
79 scenarios. Few studies have provided a planning-supporting tool which takes into account the
80 entire cascade of factors from the uncertainties of future urban rainfall behavior, to the
81 physical and economic damages resulting from extreme rainfall events, and to the
82 cost-effectiveness of alternative mitigation options, allowing for a synthesized trade-off
83 analysis of flood control solutions and pathways. This study aims to address this challenge by
84 developing such a synthesized trade-off analysis tool for supporting flood-control planning in
85 Shanghai and other growing megacities such as Shenzhen, Guangzhou, Ho Chi Minh City,
86 São Paulo, Mumbai (Bombay), Dhaka, and Jakarta.

87 Our approach follows the tradition of the bottom-up decision supporting frameworks,
88 which have a strong comparative advantage in handling deep uncertainties. Of many
89 bottom-up or robustness-based decision supporting frameworks, the following four have
90 achieved increasing popularity: Dynamic Adaptive Policy Pathway (DAPP) (Haasnoot, et al.
91 2012), Information-Gap (Info-Gap) (Ben-Haim, 2004), Robust Decision Making (Lempert
92 and McKay, 2011, Lempert et al., 2013) and Many-Objective Robust Decision Making
93 (MORDM) (Kasprzyk et al., 2013). The construction of these frameworks can be generalized
94 into the following four sequential steps: identifying decision alternatives, sampling the state
95 of affairs, specifying robustness measurements, and performing scenarios discovery to

96 identify the most important uncertainties (Hadka et al., 2015). A successful implementation of
97 these four steps is bound to be a knowledge co-creation process, which emphasizes the
98 generation of usable science for decision-making through sustained and meaningful dialogue
99 between scientists, policy makers, and other stakeholders (Clark et al., 2016; Meadows et al.,
100 2015; Liu et al., 2019). Co-creation is composed of interlinked processes of co-design and
101 co-production (Mauser et al, 2013; Voorberg et al. 2015). The former encompasses scoping of
102 broader research problems and specific project objectives and goals. It ensures that scientists
103 properly understand stakeholder needs and leads to higher stakeholder trust in project results.
104 Knowledge co-production entails the generation of new knowledge through processes that
105 integrate stakeholder and disciplinary (i.e., climate science, hydrology, economics, decision
106 science) scientific expertise. It facilitates the incorporation of stakeholder latent knowledge
107 into the overall scientific synthesis and builds stakeholder capacity to use the project
108 outcomes in decision-making (USGCRP, 2014; Clark et al., 2016).

109 In this research, we had kept sustained and meaningful dialogues with sectoral experts
110 and decision makers in each key stage of the research for the following shared purposes: (a)
111 scoping the research problems and setting project objectives and goals; (b) knowing about the
112 current protection standards, better understanding the potential vulnerabilities, and selecting
113 the right solutions; (c) finding meaningful approximate methods to grasp such complex issue
114 as the drainage capacity decrease caused by sea-level rise and land subsidence, and
115 identifying priorities and approximation margins in data-model fusion process. With the help
116 of these dialogues, we added to the upstream and midstream of the above “supply chain” the
117 entire cascade of factors that drive flood hazards and interact with the mitigation and control
118 measures. We opted to use the simple and speedy SCS Runoff Curve Number method (Chung
119 et al., 2010; Mishra and Singh, 2003; Chen et al., 2016) as the core of our inundation model
120 to bridge the gap between detailed risk assessment simulations existing in the literature and

121 the requirements of planning applications for science-informed cost-effectiveness comparison
122 across all plausible solutions. We implemented this framework to the reoccurrence scenarios
123 in the 2050s of a record-breaking extreme rainfall event in central Shanghai. To build future
124 extreme inundation scenarios, we focused on three uncertain factors, which are precipitation,
125 urban rain island effect and the decrease of urban drainage capacity caused by land
126 subsidence. To carry out a synthesized trade-off analysis of potential solutions under future
127 uncertainty, we examined the risk-reduction performance and cost-effectiveness of all
128 possible levers across different scenarios.

129

130 **1. Materials and Method**

131 **2.1. The case-study city and event**

132 Shanghai, with a territory of 6,340 km², provides residence to 24.1 million population in
133 2018. Shanghai has been the arguably most prominent economic and financial center of
134 China since the early 1900s and is now aiming to be one of the most important economic,
135 financial, shipping, and trading center of the world. However, as shown in Fig. 1, Shanghai is
136 surrounded by water on three sides, to the east by East China Sea, to the north by Yangtze
137 River Estuary, and to the south by Hangzhou Bay. In addition, Huangpu River, a tributary of
138 Yangtze River, runs through the center of Shanghai. The geological profile of Shanghai is
139 mostly composed of soft deltaic deposit. The annual rainfall is about 1200 mm/yr, with 60%
140 falling during the flooding season from May to September (He and Zhao, 2009; He, 2012;
141 Yuan et al. 2017). The analyses of He and Zhao (2009), He (2012), and Yuan et al. (2017)
142 based on daily observational records over 1981-2010 indicated that torrential rainfall
143 (cumulative precipitation > 30mm/day) in Shanghai are often intensely concentrated within a
144 period of 12 hours or less, with an occurrence frequency of 18 to 23 per year in terms of
145 five-year moving average. The five-year moving average value of extraordinary torrential

146 rainfall (cumulative precipitation > 100mm/12h) ranges one to four annually. As a
147 consequence, the most devastating hazard in Shanghai has been torrential rainfall-induced
148 inundation, which has led to transportation and other social disruptions annually, caused
149 significant economic losses and endangered urban safety. It is worth highlighting that the
150 solution district as marked in Fig. 1, which is the central business district (CBD) of Shanghai,
151 has the almost lowest elevation in comparison with other districts in the study area and in also
152 Shanghai. Therefore, the performance evaluations of flood control solutions in this study will
153 focus on this CBD area.

154

155 *(Figure 1 about here)*

156

157 Looking forward to the coming decades, global warming as a mix of rising temperatures
158 and unstable climate tends to increase the probability of heavy rainfall risks in coastal cities
159 like Shanghai (Chen et al., 2017; Jiang et al., 2015; Lee et al., 2014; Li et al. 2016; Wu et al.
160 2018). This increasing probability, combined with the trends of sea-level rise and land
161 subsidence which reduce the capacity of existing urban drainage systems, leads to a great
162 concern on the increase of the inundation risk in coastal cities by policy makers, scientists,
163 and the public. While it is recognized that the current flooding control infrastructure in
164 Shanghai would not be sufficient in defending the city against future inundation risk, there is
165 an urgent need for developing a synthesized trade-off evaluation tool to support flood-control
166 planning in Shanghai.

167 This study paid a special attention to a record-breaking event of convectional rainstorm,
168 which took place during 17-19 hours on the 13th of September 2013 and had an intensity
169 record of 130.7 mm in an hour in the study area of Shanghai (Fig. 1), being 20 mm higher
170 than the historic record in Shanghai. The event also had a sharp mark of urban rain-island

171 effect – the extreme rainfall concentrated in the study area (Fig. 1). This event caused severe
172 inundation in the main roads in Pudong CBD region and the temporary out-of-service of the
173 Century Avenue metro station, which is a hub of four metro lines. As a consequence,
174 hundreds of thousands of people were stuck during the evening rush-hour period. This
175 extreme event exposed the vulnerability of the central Shanghai in inundation risk
176 management. Therefore, it can serve as an informative baseline case for testing the impact of
177 future reoccurrence of this event on central Shanghai under a changing climate.

178

179 **2.2. Methods**

180 Fig. 2 depicts our model-coupling process across the entire cascade of factors that drive
181 flood hazards and interact with the mitigation and control measures. The first major step of
182 the process is to quantify three uncertain factors, which features the future reoccurrence of
183 the 13 September 2013 rainstorm event including spatial rain pattern and rain island effect,
184 and the decrease of urban drainage capacity. The second major step is to simulate the
185 inundation depths and areas for both the baseline event (validation of the Urban Inundation
186 Model) and each of scenario using the Urban Inundation Model. The third major step is to
187 specify various mitigation measures and to evaluate the risk-mitigation performance of these
188 measures under each inundation conditions from step 2. The fourth major step includes the
189 calculations of economic costs of various mitigation measures and then the comparative
190 analysis of cost-effectiveness of all specified mitigation measures. The rest of this section
191 will explain each of the above steps in more details.

192

193 *(Figure 2 about here)*

194

195 **2.2.1. Quantification of the three uncertain factors**

196 Observational data at 11 representative meteorological stations in Shanghai showed that

197 the number of extraordinary torrential rainfall events per year (in terms of five-year moving
198 average) did not present an obvious trend during 1960-2010. However, these data did show
199 that the extreme precipitation values (daily rainfall > 99th percentile) exhibited an increased
200 trend at all of the 11 stations, with the slope ranging between 1.31- 4.16 mm/day (also see,
201 Wang et al., 2015). We had run PRECIS 2.0 regional climate model of UK Met Office Hadley
202 Centre for the East China region with the spatial resolution of 25km under both the baseline
203 climate over 1981-2010 and the RCP4.5 scenario over 2041-2060 (denoted as the 2050s).
204 PRECIS stands for “Providing REgional Climates for Impacts Studies” and is designed for
205 researchers (with a focus on developing countries) to construct high-resolution climate
206 change scenarios for their region of interest (Hadley Centre, 2018). Representative
207 Concentration Pathway (RCP) 4.5 is a scenario that stabilizes radiative forcing at 4.5 W m^{-2}
208 (approximately 650 ppm CO_2 -equivalent) in the year 2100 without ever exceeding that value
209 (Thomson et al. 2011). The results indicate an increase of the extreme precipitation value
210 (daily rainfall > 99th percentile) by above 10% from the baseline climate to the 2050s.
211 Considering the observed historical trend in Wang et al. (2015) and the uncertainties of the
212 future climate, we assume that the increase rate (α) of the future precipitation in an
213 extraordinary torrential rainfall event in Shanghai by the 2050s will range between 7% and
214 18%, in comparison with a similar event under the baseline climate. In Section S1 of the
215 Supplementary Material, we provide more details on the estimation of this range based on
216 multiple climate model projections and RCP scenarios. In our case study of the reoccurrence
217 of the extreme rainfall event on 13 September 2013, this means that an amount of 7% to 18%
218 additional precipitation will be added to the gauge’s value of the baseline event for generating
219 more inclusive and plausible scenarios.

220 In terms of spatial distribution, Liang and Ding (2017) employed the hourly precipitation
221 records of the same 11 representative meteorological stations as employed in our research in

222 Shanghai over 1916–2014 to investigate the spatial and temporal variations of extreme heavy
223 precipitation and its link to urbanization effects. Their analysis showed that the long-term
224 trends of the frequency and total precipitation of hourly heavy rainfall across the 11 stations
225 exhibited obvious features of urban rain-island effect, with heavy rainfall events increasingly
226 focused in urban and suburban areas. In more details, the total precipitation amounts of heavy
227 rainfall event over central urban (Pudong and Xujiahui) and nearby suburban (Minhang and
228 Jiading) sites increased by the rates of 21.7-25mm/10yr. In sharp contrast, the trends at rural
229 stations are not clear and, in some cases, even show a slight reduction. Based on these
230 findings, the clear urban rain-island feature of the 13 September 2013 rainstorm event, we
231 conducted face-to-face discussions with climate experts at Shanghai Meteorological Services
232 with regard to the future dynamics of such urban island effect. The discussions came with an
233 agreement that the urban rain island effect will have a margin of increase (β_1) by 10% to 20%
234 in the case of future reoccurrence over central urban sites (Xujiahui and Pudong) by the
235 2050s, but will have a small margin of decrease (β_2) by -0.076% to -0.038% at other
236 stations.

237 With the help of above assumptions, we can establish a large set of scenarios for the
238 future reoccurrence of the extreme rainfall event on 13 September 2013. For example, by
239 taking any value within the above-assumed intervals of the increase rate of rainfall extremes
240 (α) and urban rain island effect (β_1 and β_2) respectively, we can apply these values to the
241 observed baseline precipitation amount at each of the 11 representative rain gauges to
242 generate one scenario at the gauge level. Then, we can interpolate this gauge-level scenario
243 into spatial rainfall pattern across the whole Shanghai city area.

244 Shanghai has been experiencing land subsidence for years, mostly owing to groundwater
245 extraction and increasing number of high-rise buildings. Anthropogenic urban land
246 subsidence in combination with the global warming induced sea level rise will exacerbate the

247 impact of extreme rainfall and reduce the capacity of drainage system. It is estimated that a
248 relative rise of sea level by 50cm (the height of land subsidence plus elevation of sea level
249 rise), which is highly likely by the 2050s in Shanghai, would reduce the capacity of current
250 river embankment and drainage systems by 20-30% (Liu, 2004; Wang et al., 2018). To take
251 into account the uncertainties in sea-level rise, land subsidence, and other degradation factors
252 of the drainage systems, we assume that the decreasing rate of existing drainage system
253 capability (γ) would range between 0% and 50%.

254 Dividing the intervals of α , β_1 , β_2 , and γ into 100 equal intervals would generated 10^{12}
255 combinations of plausible values of the uncertain factors, too many for a meaningful analysis.
256 To select a manageable and representative sample from these 10^{12} combinations, we
257 implemented the Latin Hyper Cube (LHC) sampling method in the R programming
258 environment. The LHC is a randomized experimental design that explores the whole input
259 space for the fewest number of representative points in sample (Lempert et al., 2013). In this
260 way, we generate 100 random scenarios of the future reoccurrence of the extreme rainfall
261 event on 13 September 2013.

262

263 **2.2.2. The Urban Inundation Model and Its Validation**

264 We developed the Urban Inundation Model (UIM) using Shanghai's data to assess urban
265 flooding risk under various extreme precipitation scenarios. There is a large number of
266 rainfall-runoff methods in the literature. Most of them require intensive input data,
267 demanding calibration, and expansive computing efforts (Chung et al., 2010; Mishra and
268 Singh, 2003). In contrast, the Soil Conservation Service Curve Number (SCS-CN), which is
269 also termed as the Natural Resource Conservation Service Curve Number (NRCS-CN)
270 method, is globally popular for its simplicity, stability, predictability, and ease of application
271 for gauged and ungauged watersheds (Chung et al., 2010; Mishra and Singh, 2003; Chen et

272 al., 2016). Given the fact that our comprehensive evaluations of thousand combinations of
273 inundation scenario and mitigation measures require for running the rainfall–runoff module
274 thousands of times, the SCS-CN method becomes the preferred choice for being the core of
275 the UIM. The UIM uses the SCS-CN urban runoff method to estimate the rainfall loss and
276 surface runoff, matched with the local elevation data and spatial urban drainage capacity. The
277 SCS-CN method is based on an empirical proportionality relationship, which indicates that
278 the ratio of cumulative surface runoff and infiltration to their corresponding potentials are
279 equal. Hooshyar and Wang (2015) provided the physical basis of the SCS-CN method and its
280 proportionality hypothesis from the infiltration excess runoff generation perspective. Chung
281 et al. (2010) amended the SCS method to allow for the theoretical exploration of the range in
282 which the CN usually falls. In Section S2 of the Supplementary Material, we provided
283 technical details of the SCS-CN method adopted in the UIM and the localization of key
284 parameters.

285 The input data required by the UIM includes: (1) gridded precipitation data, which were
286 generated by spatial interpolation of site observations (baseline) and the site-level
287 reoccurrence scenarios of the extreme rainfall event on 13 September 2013 to 30-meter
288 resolution grids. (2) Soil and land use data, which are mainly used for determining the CN
289 values of land use type, soil infiltration characteristics (soil type) and pre-soil moist condition
290 (AMC). Soil data was obtained from the Harmonized World Soil Database (HWSD) (Fischer
291 et al., 2008), with a spatial resolution of 1 km. Land use data was from the 2014 satellite data
292 inversion provided by the Institute of Geography of the Chinese Academy of Sciences, with a
293 spatial resolution of 30 meters. (3) Digital Elevation Model (DEM) elevation data, which was
294 obtained from the ASTER satellite 30-meter resolution data, using the filling process to
295 remove some false depressions according to the land use data. Considering that the residential
296 and commercial land generally have a certain step height, we made a correction on the

297 residential and commercial land terrain by adding 140mm. (4) The map of the municipal
298 underground pipe network is unavailable. However, considering that the underground
299 pipelines are typically located along the street networks, Shanghai Water Authority provided
300 drainage unit map and the approximation of the pipe capacity enclosed by streets boundaries.

301 To validate the spatial performance of the UIM's baseline simulation, we employed the
302 public-reported waterlogging point data provided by the Shanghai Police Office on Sep 13th
303 2013. This database showed 760 reported flood points during 17-19 hours on the 13th of
304 September 2013 and most of them were in the solution district of our Study area. Fig. 3
305 compares the spatial patterns of simulated inundation by the UIM and the public-reported
306 waterlogging points. It shows a very good match in terms of area coverage in the solution
307 district.

308

309 *(Figure 3 about here)*

310

311 To further check the accuracy of the UIM simulation in terms of water depth, we ran
312 InfoWorks (v 8.5, developed by Innowyze, 2018; Han, 2014; Han et al. 2014) simulation of
313 the same event for the same solution district using the same input data in the UIM
314 hydrological module. InfoWorks ICM is an integrated catchment modeling software and has
315 been widely used in urban flooding simulations in the business world. The InfoWorks ICM
316 enables to create an integrated model for 1D hydrodynamic simulations and 2D simulations
317 both above and below ground drainage networks in urban area. The 1D and 2D integration
318 model gives a holistic view of complete catchment as it happens in reality, and many works
319 were generated in a small spatial zone as a number of blocks or a community. However, its
320 triangle based 2D mesh zone sacrifices the calculation speed at a city district level. In our test,
321 the ground model (DEM) was meshed in 2D Zone with triangle unit area between 1000m² to

322 5000m², and the different drainage unit is modeled in different infiltration surface considering
323 their drainage capacity. The comparison statistics shows that both the UIM and InfoWorks
324 ICM simulations have the similar maximum depths (840mm versus 800mm) and similar size
325 of inundated area (20 km² versus 21 km²).

326

327 **2.2.3. Characteristics of Solutions**

328 Although Shanghai has already built up a comprehensive flood and inundation protection
329 system, additional solutions are still needed to address the inundation issue in the future.
330 Aiming to increase the current protection standards, a series of hydraulic engineering projects
331 have been planned or are under construction, which includes the upgrading of old drainage
332 pipelines, construction of deep tunnels under the riverbed of the lower reach of Suzhou Creek,
333 and other green infrastructure projects. In line with the 13th five-year plan of Shanghai on
334 flooding control (Shanghai Municipal Government, 2017) and the ongoing hydrological
335 engineering projects, we evaluate three sets of solutions, the increase in the capacity of
336 drainage systems by the planned rates, the increase of green area by various rates, and the
337 construction of deep tunnels with varying capacities. To make these solutions geographically
338 compatible, we assume all the solutions are implemented in the same core region within the
339 study area (i.e., the solution district), which is about 70km² and mainly consist of the core
340 CBD region in Shanghai.

341 *Drainage.* The study area is divided into 284 drainage units by Shanghai Water Authority.
342 These units are categorized by three types of standards in terms of drainage capacity: 27mm/h,
343 36mm/h and 50mm/h, based on the current designed capacity of local return period of 1, 2,
344 and 5 years. According to the 13th five-year plan for water management and flood control in
345 Shanghai (Shanghai Municipal Government, 2017), the current drainage standard will be
346 raised in central Shanghai. Following this plan and consultations with water and urban

347 planning authorities, we assume that the drainage capacity in the whole solution district will
348 be upgraded to the highest standard: 50mm/h. This means that the extent of standard rising is
349 location specific.

350 *Green Area.* The Shanghai Municipal Government has shown a strong willingness to
351 improve the urban ecological environment through augmented funding for preserving and
352 expanding public green areas. Statistical data show that both urban green area coverage and
353 forest coverage have been increasing annually in last 25 years (Statistical Yearbook of
354 Shanghai, various years). It is anticipated that future investment in green area will continue to
355 rise. In addition to their great contribution to air cleaning and urban environmental
356 improvement, green areas also play an important role in rain-water harvesting and reducing
357 urban surface runoff. The Municipal Government has strongly promote “sponge city”
358 guideline of increasing the green and permeable area by building green roofs and porous
359 pavement, and by tree and grass planting in public spaces. In line with this guideline and
360 Shanghai Master Plan 2017-2035 (Shanghai Urban Planning and Land Resource
361 Administration Bureau, 2018), we assume that about 40% of the existing impermeable and
362 moderately permeable (with 50% permeability) area in the Solution District, equivalent to
363 about 30km², will become permeable (with 70% permeability) by the 2050s. We down-scale
364 the district-specific requirements of the “sponge city” guideline and Master Plan onto the
365 drainage unit level. This means that the distribution of the green area is specific to each
366 drainage unit, but there is no locational alternatives. The conversion from the impermeable
367 area and moderately permeable to permeable is modelled in the UIM through changes in the
368 CN. In more detail, the permeability conversion is implemented by lowering the values of CN
369 in the SCS model from 98 and 86 to 80 in the corresponding areas.

370 *Deep tunnel.* The construction of deep tunnels will increase the urban capacity to
371 minimize the surface runoff and thus reduce the inundation impact. Shanghai initiated the

372 Suzhou Creek deep tunnel project in 2016 with a designed length of 15.3km, which aims to
373 serve an area of 58 km² mostly in the study area. The target of the deep tunnel is to raise the
374 drainage standard from 1 year to 5 years return period in its serving area and to well manage
375 the rainstorm with a 100 year return period, bringing no regional transportation abruption and
376 keeping the water depth on roads no more than 15cm. The first stage of the project is planned
377 to be completed by the end of 2020, followed by the construction of supporting systems (2nd
378 stage), and then long-term extension stage. Given the fact that construction of a complete
379 system of deep tunnel water storage, sedimentation and purification, and discharge by
380 pumping is financially expansive and time consuming, we designed to test three levels of the
381 capacity of the deep tunnel project: handling 30%, 50% and 70% (Tun30, Tun50, and Tun70)
382 of remaining floodwater after those handled by the existing infrastructure in the baseline run
383 of the UIM (the rainfall event on 13 September 2013). These three levels of capacity are
384 equivalent to satisfactorily serving an area of 21km², 35km², and 49km² with the standard of
385 5-year return period in the solution district, respectively.

386

387 **2.2.4. Performance Evaluation**

388 For each solution or a combination of solutions, we evaluate its beneficial performance by
389 the metric of the risk reduction rate (RRR). The hydrological effectiveness (as measured by
390 the RRR) per unit of abatement cost is employed to evaluate the cost-effectiveness of
391 different solutions.

392 Flood-induced casualties and physical damage to buildings, indoor/outdoor belongings,
393 infrastructure and natural resources constitute the direct loss, which, in general, can be
394 measured definitely by monetizing across all assets. Damage incurred by a physical asset was
395 calculated as a percentage of its value, and the function relating flood depths to this
396 proportion is called a depth-damage curve, which considers the relationships of flood

397 characteristics (such as water depth, flow velocity, flood duration, etc.) and damage extent
 398 (either by the absolute damage values or the relative damage rates) in the elements at risk.

399 The study area is located in the CBD with a high density of residential and commercial
 400 properties. We opted to focus on direct damage loss resulting from inundation. Loss caused
 401 by the possibility of structural damage from the velocity of incoming water is not estimated.
 402 In other words, we specifically look at the categories of damage to buildings (residential,
 403 commercial), loss of belongings (indoor) and economic disruption so as to examine the direct
 404 losses caused by urban inundation. We evaluated the inundation risk based on the following
 405 equation (ISO Guide 31000, 2009).

$$406 \quad Risk = Hazard \times Exposure \times Vulnerability. \quad (1)$$

407 Section S3 in Supplementary Material presents the procedures to quantify each element in
 408 Eq. (1). The risk reduction rate (RRR) by a specific set of mitigation solutions is calculated as
 409 the percentage difference between the risk under the given extreme-rainfall scenario without
 410 adding any solution (R_N , “not treated”) and the risk under the same extreme-rainfall scenario
 411 with the specific set of solutions (R_T , “treated”) as specified in Eq. (2).

$$412 \quad RRR = \frac{R_N - R_T}{R_N} \times 100\%. \quad (2)$$

413 Benefit-cost ratio is often used in public investment analysis. However, it is not easy to
 414 accurately quantify the public benefits of inundation abatement. In contrast, the
 415 cost-effectiveness, which measures the hydrological effectiveness per unit of abatement cost,
 416 can be quantified with confidence and can serve the purpose of comparison across different
 417 scenario-solution combinations (Chui et al., 2016; Liao et al., 2013). We use the RRR from
 418 Eq. (2) to measure the hydrological effectiveness. For cost estimation, a life cycle cost
 419 analysis is necessary because the solutions differ in initial cost, annual operation and
 420 maintenance cost, salvage value and particularly, lifespan. We calculate the present value (in
 421 2013 RMB) of the life cycle cost of a solution (or a combination of solutions). In the

422 calculation, we assume that the discount rate in Shanghai is 5% as justified in Ke (2015).
423 Section S4 in Supplementary Material presents more information on cost estimations of the
424 basic solutions.

425

426

427

428 **3. Result**

429 **3.1. Inundation Simulation**

430 The 100 sampled scenarios of the future reoccurrence of the 13 September 2013 rainstorm
431 event, as selected in Section 2.2.1, were simulated based on the current flood control
432 infrastructure in the whole study area (reference runs). Two indexes were presented herewith
433 to show the uncertain extent of the inundation: (1) average inundation depth in the solution
434 district, and (2) the average 90th percentile depth, which features the average depth of the
435 upper decile of the most inundated drainage units within the solution district.

436 Fig. 4 shows the variation across the 100 scenarios. It appears that the second index
437 increases in direct correspondence to the first one. The maximum and minimum of both
438 indicators arrive in Sc-11 and Sc-53, with the maximum and minimum of the first index being
439 97.68mm and 17.65mm, and those of the second being 543.2mm and 176.5mm, respectively.
440 The variation of the average inundation across the 100 scenarios are large and its minimum is
441 only 18% of its maximum, whereas the minimum of average 90th percentile inundation equals
442 67.5% of its maximum.

443

444 *(Figures 4 and 5 about here)*

445

446 All scenarios add increments to both the baseline inundation depth and area. Sc-11, Sc-3

447 and Sc-53 show the worst, moderate and mild increments (Fig. 5). The hotspot inundation
448 areas are mostly in the CBD region where agglomerations of numerous properties and
449 business are located along the banks of the Huangpu River. The affected area in Sc-11 is
450 significant large than that in both Sc-3 and Sc-53. In terms of inundation depth, many grids in
451 Pudong District show high values in all three scenarios. In the worst case Sc-11, the
452 inundation depth reaches as high as 1420mm in some grids in Pudong, which is 750mm
453 higher than the maximum depth in the baseline simulation, and the inundated area is more
454 than doubled in comparison with the baseline. Even in mild increment scenario like Sc-11,
455 there are still some grids in the CBD region where the average 90th percentile water depth can
456 be more than 1000mm, implying a high potential risk in the 2050s (Fig.5).

457

458 **3.2. The performance of Solutions in Reducing Inundation**

459 To evaluate the performance of solutions in reducing inundation, we re-run the
460 simulations of the 100 sampled scenarios based on the following five flood control solutions
461 and their various combinations in the solution district: drainage capacity enhancement
462 (drainage), green area increase (green), deep tunnel with 30% runoff absorbed (Tun30), deep
463 tunnel with 50% runoff absorbed (Tun50), deep tunnel with 70% runoff absorbed (Tun70). A
464 performance evaluation based on average depth and average 90th percentile depth shows that:
465 1) most of the solutions perform well in the mild increment cases (e.g. Sc-53), in which the
466 solutions can wipe out the inundation water generally; (2) in the worst rainfall increment
467 cases (e.g. Sc-11), the performance of solutions varied from good to very poor; 3) the depth
468 reduction range of all solutions across the 100 rainfall scenarios is from 8% (e.g., “drainage”
469 in Sc-11) to 98.9% (e.g. Tun50, “Drainage”+“Green”+Tun30, and Tun70 in Sc-53).

470 Because of the heavy precipitation (more than 140mm) in a short duration (less than 3
471 hours), and in addition, the decrease of the drainage capacity (γ) caused mainly by sea-level

472 rise and land subsidence, the drainage improvement solution alone is unable to meaningfully
473 reduce the water level in most cases, especially in the worst cases. A key aspect of the
474 “sponge city” is to increase green area which can in turn increase the rainwater infiltration
475 and residence time. However, increased green space alone does not perform well in the worst
476 increment scenario as well. The implementation of a deep tunnel solution shows an advantage
477 in reducing the surface runoff, especially during a rainfall peak by absorbing 30%, 50% and
478 70% of remaining runoff after the absorption in the baseline UIM run. By combining
479 different solutions together, we find that the combination of green area and drainage is able to
480 improve the performance in the worst-case scenario and the performance increases
481 significantly once adding the deep tunnel solutions in.

482 The risk reduction rate (RRR) by a specific set of solutions from the risk level under an
483 extreme-rainfall scenario without adding any solution is calculated using Eq. (2) to determine
484 the performance of this set of solutions. Fig. 6 shows the RRRs of seven selected solutions –
485 green area increase (GA), drainage enhancement (Dr), Tun30, Dr + GA (D+G), Tun50, Dr +
486 GA + Tun30 (D+G+Tun30), and Tun70 – under each of the 100 rainfall scenarios, with
487 reference to different level of γ , the parameter featuring the uncertainties in the decreasing
488 rate of existing drainage system capability caused by sea-level rise, land subsidence, and
489 other degradation factors. Fig. 6 also shows the average inundation depth across the
490 combinations of solution and rainfall scenarios at the given level of γ . In Fig. 6 we can see
491 that the average inundation depth increases almost linearly with the reduced drainage
492 capacity (γ) and furthermore there is a strong negative correlation between the average
493 inundation depth and the risk reduction rates of any given set of solutions when moving with
494 γ . In fact, similar strong negative correlation also exists between the average inundation depth
495 and risk reduction rate of any a given combination of solution and rainfall scenario when
496 moving along the γ axis. By contrast, the correlation between future precipitation and the

497 inundation depth is much weak. This set of results indicates that drainage capacity decrease
498 caused by sea-level rise and land subsidence will play a dominant role in worsening future
499 inundation risks in Shanghai.

500 Fig. 7 displays the box plots of the RRR results over seven selected sets of solutions. It
501 shows that the RRR performances of the first two solutions, i.e. “drainage capacity
502 enhancement” and “green area increase”, are the lowest in comparison with other solutions
503 and are statistically similar. The third and fourth solutions, i.e., “deep tunnel with 30% runoff
504 absorbed” and “drainage enhancement + green area expansion,” are able to reduce the
505 inundation risk by a large margin on average, but their performances are very dispersed with
506 poor performances in the worst case scenarios. The remaining three solutions, i.e., “deep
507 tunnel with 50% runoff absorbed”, “drainage enhancement + green area expansion + deep
508 tunnel with 30% runoff absorbed”, and “deep tunnel with 70% runoff absorbed”, are much
509 better performers and the performances of the last two solutions are statistically reliable even
510 in the worst case scenarios.

511

512 *(Figures 6 and 7 about here)*

513

514 **3.3. Cost-effectiveness Comparison**

515 Table 1 presents the comparative cost structure of the five basic solutions. The cost is
516 accounted as the present value in 2013 RMB. The annual average cost (AAC) in the table
517 indicates that the low impact solution of “green area expansion” has the lowest financial
518 demand per year and the highest impact grey solution of Tun70 has the highest financial
519 demand per year, respectively. Table 2 compares the cost-effectiveness of the above five basic
520 solutions and the two combinations of “drainage enhancement + green area expansion” (D+G)
521 and “drainage enhancement + green area expansion + deep tunnel with 30% runoff absorbed”

522 (D+G+Tun30). Because the effectiveness measure in the comparison focuses on the risk
523 reduction rate, the comparison clearly puts higher values on the deep tunnel solutions, of
524 which Tun50 has the highest effectiveness-cost ratio. If the criterion of solution choice is that
525 the risk reduction rate should be at least 85% on average, Tun70 will have the highest
526 effectiveness-cost ratio.

527

528 (*Tables 1 and 2 about here*)

529

530 **4. Discussion**

531 This study has proposed a planning-supporting tool which is capable of considering the
532 entire cascade of factors from the uncertainties of future urban rainfall pattern and intensity,
533 to the physical and economic damages caused by extreme rainfall events, and to the
534 cost-effectiveness comparison of plausible solutions. The application of this synthesized
535 trade-off analysis tool to the case of the reoccurrence in the 2050s of the extreme rainfall
536 event on 13 September 2013 in Shanghai reveals a number of findings which are informative
537 to urban planners and other stakeholders. First, the results show that drainage capacity
538 decrease caused by sea-level rise and land subsidence will contribute the most to the
539 worsening of future inundation risk in Shanghai. In contrast, future precipitation and urban
540 rain island effect will have a relatively moderate contribution to the increase of the inundation
541 depth and area. This result is also indirectly supported by a real rainstorm event happened in
542 June 2015, which caused severe inundation in central Shanghai for days because high water
543 level of rivers in the region prevented rainwater pumping from sewer systems into the river
544 system. This finding should have general implications for other coastal cities sitting on river
545 mouth. It means that it is important for urban planners in those cities to consider a scenario of

546 a compound event in which an extreme storm surge under a sea level rise background takes
547 place in an astronomical high tide period. Such an event would cause very severe flooding
548 inside the city and bring disastrous impacts. To avoid regret in the near future, the mitigation
549 and adaptation solutions should pay great attention to drainage standard increasing and
550 drainage capacity strengthening, which should be ahead of the pace of sea level raise plus
551 land subsidence.

552 The cost-effectiveness comparison in Section 3.3 brings up an important decision-making
553 issue on the trade-offs between the grey infrastructure and the green solutions. The latter is
554 usually known by varying names in different cultures, e.g. Low Impact Development (LID)
555 in the US, Sustainable Urban Solutions (SUDS) in the UK, and Sponge City in China. The
556 grey infrastructure usually possesses better protection standards in reducing inundation risks
557 associated with the low return period events, but has a high level of negative impact on
558 ecology and such negative impact is very difficult to be quantified. In sharp contrast, green
559 solutions are typically effective in managing relatively high return period events, but
560 beneficial to the local environment and ecology and such benefits are very difficult to be
561 measured by monetary value (Palmer et al., 2015). Because it is difficult to measure the
562 negative impact of grey infrastructure and the positive benefits of green solutions to the
563 environment, planners typically under estimate both of them by a large margin. In recognition
564 of this limitation, the solution of “drainage enhancement + green area expansion + deep
565 tunnel with 30% runoff absorbed” (D+G+Tun30) becomes preferable to the solution of “deep
566 tunnel with 70% runoff absorbed” (Tun70), given the integrative effect of D+G+Tun30 in
567 reducing urban inundation risk by 85% ($\pm 8\%$) and in improving the local air quality and
568 micro-climate.

569 Synthesized trade-off analysis of flood control solutions under future deep uncertainty
570 asks for consolidation of various sets of data from different sources and for decision-making

571 by the researchers in terms of solving conflicts across data sets and data sources, finding
572 proxies for missing data, and identifying priorities and approximation margins in data-model
573 fusion process. Our decisions on these important issues were made jointly with local experts
574 and policy makers in a knowledge co-production process (Clark et al., 2016; Lempert, et al.
575 2013; Liu et al., 2019; USGCRP, 2014). Field surveys and focus-group discussions were
576 applied in the early stage of this work, which provided very useful information for knowing
577 about the current protection standards, for illuminating the potential vulnerabilities, and for
578 selecting the right adaptation solutions. Opinions of experts from different infrastructure
579 sectors and scientific fields and discussions with stakeholders and policy makers also gave us
580 inspiration for this Shanghai inundation application (Sun et al. 2019). For instance, expert
581 opinions provided valuable insight for estimating the relationship between the drainage
582 capacity and river water level and for using this relationship to approximate the drainage
583 capacity decrease caused by sea-level rise and land subsidence. Discussions with policy
584 makers and other stakeholders enabled us to know better their interests and priorities, which
585 motivated our choices of solutions and key sources of uncertainties. This knowledge
586 co-creation process also led to high trust in project results by policy makers. The results of
587 the work were delivered to local decision-making authorities. Both the findings and the tool
588 for the synthesized trade-off analysis of flood control solutions under future deep uncertainty
589 were well appreciated by the authorities.

590 With increased demand for wise and visionary decisions in dealing with the risk and
591 uncertainties posed by future climate change, there is an urgency to bridge the gap between
592 the scientific research and practical applications. Although there is a myriad of research
593 running flood risk simulations and assessments in Shanghai and other mega-cities in the
594 coastal areas, seldom can the detailed quantified solutions be digested by planners. This work,
595 by integrating the simple but speedy SCS-CN based hydrological model into the framework

596 of robust decision making under deep uncertainty, provides a practical and instructive
597 example for bridging this important gap.

598

599 **5. Conclusion**

600 Precipitation change in the future is subject to deep uncertainties, especially in coastal
601 mega-cities like Shanghai. Long-term planning to manage flood risk caused by extreme
602 rainfall events is challenged by uncertainty in precipitation change and also in socioeconomic
603 changes and contested stakeholder priorities. In this paper, we have proposed an integrated
604 framework for a synthesized trade-off analysis of multiple flood-control solutions under the
605 condition of deep uncertainties. We have demonstrated its operational ability with an
606 application case study of central Shanghai, which focused on the reoccurrence in the 2050s of
607 the extreme rainfall event on 13 September 2013. In the case study, we considered three
608 uncertain factors, which include precipitation, urban rain island effect, and the decrease of
609 urban drainage capacity caused by land subsidence and sea level rise. We built future extreme
610 inundation scenarios based on the plausible ranges of changes in the above three uncertain
611 factors and randomly selected 100 scenarios by using the Latin Hyper Cube (LHC) sampling
612 method. We then estimated the inundation depth and area of these 100 rainfall scenarios
613 under the condition of both existing infrastructure (reference runs) and enhanced
614 infrastructure by introducing alternative sets of inundation-control solutions (“treated” runs).
615 The inundation-control solutions include the increase of public green area, raising the
616 standards of urban drainage system, construction of deep tunnel with varying levels of
617 capacity, and the various combinations of the above basic solutions. The direct physical
618 losses were calculated for the 100 reference runs and also for all “treated” runs, based on the
619 depth-damage curves. The resultant large set of simulation results enabled us to calculate and
620 then compare the risk-reduction performances of all possible solutions in different rainfall

621 scenarios.

622 Two key results of these simulations and analyses are worth highlighting. First, drainage
623 capacity decrease caused by sea-level rise and land subsidence will play a dominant role in
624 worsening future inundation in central Shanghai. This finding in combination with others
625 urges future infrastructure planning in coastal cities to pay a great attention to the compound
626 event of an extreme storm surge under a sea level rise background occurring in a period of
627 astronomical high tide. A “no regret” planning should be pro-active by strengthening the
628 drainage capacity well ahead of the pace of sea level raise plus land subsidence. Second,
629 although a performance comparison with a “flooding risk reduction rate” focus puts the
630 solution of “deep tunnel with 70% runoff absorbed” (Tun70) ahead of “drainage enhancement
631 + green area expansion + deep tunnel with 30% runoff absorbed” (D+G+Tun30), a
632 consideration that the negative impact associated with deep tunnel construction on the
633 environment and the environmental benefits of green areas are typically underestimated puts
634 D+G+Tun30 as the top choice, which can reduce the future flood risk by 85% ($\pm 8\%$). This
635 example enriches the literature on the performance evaluations between grey (e.g. traditional
636 engineering structure) and green solutions in mitigating urban flood risk with reference to
637 financial and ecological benefits and costs.

638 The experience of this research suggests that a synthesized trade-off analysis of
639 alternative flood control solutions under future deep uncertainty cannot be accomplished by
640 scientists alone, and it must be a knowledge co-creation process with decision makers and
641 field experts. Such a knowledge co-creation process can ensure usable science for
642 decision-making and lead to higher trust in project results by policy makers. Of course, the
643 advantage of our decision supporting tool in running comprehensive evaluations for thousand
644 combinations of scenarios-measures within a one or few days and with moderate demand for
645 input data implies its disadvantage in lack of details at the grid-cell level. The second

646 limitation is that the risk assessment in our work considered only the direct losses caused by
647 inundation and ignored the indirect losses like interruptions to transportation and other urban
648 functions, and then the sequential chain effect across urban social and economic sectors.

649

650

651 **Acknowledgement**

652 This work was sponsored by the National Natural Science Foundation of China (Grant
653 Nos.51761135024, and 41671113), the Engineering and Physical Sciences Research Council
654 of UK (Grant Nos. R034214/1), the Netherlands Organization for Scientific Research (NWO)
655 (Grant Nos. ALWSD.2016.007), and the UK-China Research & Innovation Partnership Fund
656 through the Met Office Climate Science for Service Partnership (CSSP) China as part of the
657 Newton Fund (Grant Nos. AJYG-643BJQ). We gratefully acknowledge the valuable advices
658 from Prof. Robert Lempert and Prof. Steven Popper of RAND Corporation. We thank
659 Hanqing Xu for excellent research assistance. Hengzhi Hu thanks the START program to
660 sponsor his attendance at the RDM training workshop and visit to Rand Corporation.

661

662

663

664 **Reference**

665 Aerts, J.C.J.H., Botzen, W.J.W., Emanuel, K., et al. 2014. Evaluating flood resilience strategies for
666 coastal megacities. *Science* 344 (6183), 473-475.

667 Aerts, J.C.J.H., Lin, N., Botzen, W.J.W., Emanuel, K., de Moel, H. 2013. Low-Probability Flood Risk
668 Modeling for New York City. *Risk Analysis*: 1-17.

669 Chen, H.-P., Sun, J.-Q., Li, H.-X. 2017. Future changes in precipitation extremes over China using the
670 NEX-GDDP high-resolution daily downscaled dataset. *Atmospheric and Oceanic Science Letters*,
671 10(6), 403-410. DOI: 10.1080/16742834.2017.1367625.

672 Chen, Y., Samuelson, H.W., Tong, Z. 2016. Integrated design workflow and a new tool for urban

- 673 rainwater management. *J. Env. Manag.* 180, 45-51.
- 674 Chui, T.F.M, Liu, X., Zhan, W. 2016. Assessing cost-effectiveness of specific LID practice designs in
675 response to large storm events. *J. Hydrology* 533, 353–364.
- 676 Chung, W. H., Wang, I.T., Wang, R.Y. 2010. Theory-based SCS-CN method and its applications. *J*
677 *Hydrol Eng* 15(12):1045–1058.
- 678 Clark, W. C., van Kerkhoff, L., Lebel, L., & Gallopin, G. C. 2016. Crafting usable knowledge for
679 sustainable development. *Proc. Natl. Acad. Sci. Unit. States Am.*, 113 (17), 4570-4578.
- 680 CRED (Centre for Research on the Epidemiology of Disasters), (2014), EM-DAT—The International
681 Disaster Database.
- 682 Fan, F. L., Deng, Y. B., Hu, X. F. et al., 2013. Estimating composite curve number using an Improved
683 SCS-CN Method with Remotely Sensed Variables in Guangzhou, China. *Remote Sensing*, 5(3):
684 1425–1438.
- 685 Fischer, G., Nachtergaele, F., Prieler, S., et al., 2008. Global Agro-Ecological Zones Assessment for
686 Agriculture (GAEZ 2008). IIASA, Laxenburg, Austria and FAO, Rome, Italy.
- 687 Gu, W., Tan, J.-G., Chang, Y.-Y. 2015. Characteristics of heavy rainfall event in Shanghai region from
688 1981-2013. *J. Met. Env.* 31(6), 107-114.
- 689 Haasnoot, M., Middelkoop, H., Offermans, A., Beek, E.V., Deursen, W.P.A.V., 2012. Exploring
690 pathways for sustainable water management in river deltas in a changing environment. *Climatic*
691 *Change* 115, 795–819.
- 692 Hadka, D., Herman, J., Reed, P., Keller, K., 2015. An open source framework for many objective
693 robust decision making. *Environ. Model. Softw.* 74, 114–129.
- 694 Hadley Centre, 2018. PRECIS: a regional climate modelling system.
695 <https://www.metoffice.gov.uk/research/applied/international/precis>.
- 696 Hallegatte, S., Green, C., Nicholls, R.J., Corfee-Morlot, J., 2013. Future flood losses in major coastal
697 cities. *Nat. Clim. Change* 3, 802–806.
- 698 Han, J. C., 2014. Optimization of upgrading schemes of drainage systems by InfoWorks ICM
699 software. *China Water & Wastewater*. 30(11) 34-38.
- 700 Han, J.-Y., Baik, J.-J., Lee, H., 2014. Urban impacts on precipitation. *Asia-Pac. J. Atmos. Sci.* 50,

- 701 17-30.
- 702 He, B., Chen, C., Zhou, N. 2003. Urbanized area runoff coefficient and its application. Shanghai
703 Environmental Science 22(7), 472-476. (In Chinese)
- 704 He, F.F., Zhao, B.K. 2009. The characteristics of climate change of torrential rains in Shanghai region
705 in recent 30 years. Adv. Earth Sci. 24, 1260–1267. (In Chinese)
- 706 He, F.F. 2012. Characteristics of torrential rain in Shanghai from 1980s. In Proceedings of the Urban
707 Meteorology Forum—Urban and Climate Change, Shenzhen, China, 24–25 November 2012; pp.
708 10–17. (In Chinese)
- 709 Hooshyar, M., Wang, D. 2016. An analytical solution of Richards' equation providing the physical
710 basis of SCS curve number method and its proportionality relationship, Water Resour. Res., 52,
711 6611–6620, doi:10.1002/2016WR018885.
- 712 Huong, H. T. L., Pathirana, A. 2013. Urbanization and climate change impacts on future urban flood
713 risk in Can Tho city, Vietnam. Hydrol. Earth Syst. Sci. 17, 379–394.
- 714 Innovyze, 2018, InfoWorks ICM is an advanced integrated catchment modeling software.
715 <https://www.innovyze.com/en-us/products/infoworks-icm>.
- 716 ISO Guide 31000, 2009. Risk management - Principles and guidelines.
717 <http://ehss.moe.gov.ir/getattachment/56171e8f-2942-4cc6-8957-359f14963d7b/ISO-31000>.
- 718 IPCC. Climate change 2014: impacts, adaptation, and vulnerability [M]. Cambridge: Cambridge
719 University Press.
- 720 Jenkins, K., Surminski, S., Hall, J., et al. 2017. Assessing surface water flood risk and management
721 strategies under future climate change: Insights from an agent- based model. Science of the Total
722 Environment 595, 159-168.
- 723 Jiang, Z. H., Li, W., Xu, J., et al. 2015. Extreme precipitation indices over China in CMIP5 models.
724 Part I: Model evaluation. Journal of Climate 28(21), 8603-8619.
- 725 Ke, Q. 2014. Flood Risk Analysis for Metropolitan Areas – A Case Study for Shanghai. PhD
726 Dissertation, Technology of Delft University, Department of Hydraulic Engineering.
- 727 Kharin, V. V., F. W. Zwiers, X. Zhang, and G. C. Hegerl (2007), Changes in temperature and
728 precipitation extremes in the IPCC ensemble of global coupled model simulations, J. Clim., 20(8),

- 729 1419–1444.
- 730 Kusaka, H., Nawata, K., Suzuki-Parker, A., Takane, Y. & Furuhashi, N. (2014), Mechanism of
731 precipitation increase with urbanization in Tokyo as revealed by ensemble climate simulations. *J.*
732 *Appl. Meteorol. Climatol.* 53, 824–839.
- 733 Lee, J.W., Hong, S.Y., Chang, E.C., et al. 2014. Assessment of future climate change over East Asia
734 due to the RCP scenarios downscaled by GRIMs-RMP. *Climate Dynamics* 42(3–4), 733–747.
- 735 Lempert, R.J., Groves, D.G., 2010. Identifying and evaluating robust adaptive policy responses to
736 climate change for water management agencies in the American west. *Technol. Forecast. Soc.*
737 *Chang.* 77, 960–974.
- 738 Lempert, R. J., Kalra N, Peyraud S, 2013. Ensuring Robust Flood Risk Management in Ho Chi Minh
739 City. RAND, Santa Monica, CA.
- 740 Lempert, R J, McKay, S. 2011. Some thoughts on the role of robust control theory in climate-related
741 decision support. *Climate Change.* 2011(107): 241-246.
- 742 Li, W., Jiang, Z., Xu, J., et al. 2016. Extreme Precipitation Indices over China in CMIP5 Models. Part
743 II: Probabilistic Projection. *Journal of Climate* 29(24), 8989-9004.
- 744 Liang, P., Ding, Y. H. 2017. The long-term variation of extreme heavy precipitation and its link to
745 urbanization effects in Shanghai during 1916–2014. *Advances in Atmospheric Sciences*, 34, 321–
746 334.
- 747 Liao, Z.L., He, Y., Huang, F., Wang, S., Li, H.Z. 2013. Analysis on LID for highly urbanized areas’
748 waterlogging control: demonstrated on the example of Caohejing in Shanghai. *Water Science &*
749 *Technology,* 68 (12), 2559- 2567.
- 750 Liu, D.-G. 2004. Possible impacts of relative sea level rise in the coastal areas in China. *Marine*
751 *Forecasts* 21(2), 21-28 (in Chinese).
- 752 Liu, J., Bawa, K. S., Seager, T. P., Mao, G., Ding, D., Lee, J. S. H., Swim, J. K., 2019. On knowledge
753 generation and use for sustainability, *Nature Sustainability* 2: 80-82.
- 754 Löwe, R., Urich, C., Domingo, N., et al. 2017. Assessment of urban pluvial flood risk and efficiency
755 of adaptation options through simulations – A new generation of urban planning tools. *Journal of*
756 *Hydrology.* 355-367.

- 757 Mauser, W., Klepper, G., Rice, M., Schmalzbauer, B. S., Hackmann, H., Leemans, R., & Moore, H.
758 (2013). Transdisciplinary global change research: the co-creation of knowledge for sustainability.
759 *Current Opinion in Environmental Sustainability*, 5(3-4), 420-431.
- 760 Meadow, A. M., Ferguson, D. B., Guido, Z., Horangic, A., Owen, G., Wall, T. 2015. Moving toward
761 the deliberate coproduction of climate science knowledge. *Weather, Climate, and Society*, 7(2),
762 179-191.
- 763 Mishra, S. K., Singh, V. P. 2003. Soil conservation service curve number (SCS-CN) methodology.
764 Kluwer Academic Publishers, Dordrecht.
- 765 Mishra, V., Lettenmaier, D. P. 2011. Climatic trends in major US urban areas, 1950–2009, *Geophys.*
766 *Res. Lett.*, 38, L16401, doi:10.1029/ 2011GL048255.
- 767 Muis, S., Güneralp, B., Jongman, B., Aerts, J. C. J. H., Ward, P. J. 2015. Flood risk and adaptation
768 strategies under climate change and urban expansion: a probabilistic analysis using global data.
769 *Science Total Environ.* 538, 445–457.
- 770 Palmer, M.A., Liu, J., Matthews, J.H., Mumba, M., D’Odorico, P., 2015. Manage water in a green way.
771 *Science* 349 (6248): 584-585.
- 772 Paul, S., Ghosh, S., Mathew, M., Devanand, A., Karmakar, S., Niyogi, D. 2018. Increased spatial
773 variability and intensification of extreme monsoon rainfall due to urbanization. *Sci. Rep.* 8, 3918.
- 774 Poelmans, L., von Rompaey, A., Ntegeka, V., Willems, P. 2011. The relative impact of climate change
775 and urban expansion on peak flows: a case study in central Belgium. *Hydrol. Process.* 25, 2846–
776 2858.
- 777 Rosenzweig, C., Solecki, W. D., Hammer, S. A., Mehrotra, S. 2011. *Climate Change and Cities: First*
778 *Assessment Report of the Urban Climate Change Research Network*. Cambridge University
779 Press, Cambridge, UK.
- 780 Sekovski, I., Armadorim C., Calabrese, L., Mancini, F., Stecchi, F., Perini, L. 2015. Coupling
781 scenarios of urban growth and flood hazards along the Emilia-Romagna coast (Italy). *Nat.*
782 *Hazards Earth Syst. Sci.* 15, 2331–2346.
- 783 Shanghai Climate Change Annual Bulletin, 2014, 2016. Shanghai Climate Center. In Chinese.
- 784 Shanghai Municipal Government. 2017. The 13th Five-year Plan of Shanghai on Water Resource

- 785 Protection and Utilization and Flooding Control. Available (in Chinese) at
786 <http://fgw.sh.gov.cn/wcm.files/upload/CMSshfgw/201706/201706050327041.pdf>.
- 787 Shanghai Urban Planning and Land Resource Administration Bureau. 2018. Shanghai Master Plan
788 2017-2035. The version for public reading is available at:
789 <http://www.shanghai.gov.cn/newshanghai/xxgkfj/2035004.pdf>.
- 790 Shanghai Water Engineering Design & Research Institute, 2011. Suzhou Creek Water Gate
791 Engineering. in Chinese
- 792 Shimoju, R., Nakayoshi, M., Kanda, M. 2010. Case analyses of localized heavy rain in Kanto
793 considering urban parameters (in Japanese with English abstract). *Ann. J. Hydraul. Eng.*, 54,
794 349–354.
- 795 Souma, K., Tanaka, K., Suetsugi, T. et al. 2013. A comparison between the effects of artificial land
796 cover and anthropogenic heat on a localized heavy rain event in 2008 in Zoshigaya, Tokyo, Japan,
797 *J. Geophys. Res. Atmos.*, 118, 11,600–11,610, doi:10.1002/jgrd.50850.
- 798 *Statistic Year Book of Shanghai, 2013, 2014, 2015.* Shanghai Statistics Bureau. In Chinese.
- 799 Sun, Landong, Tian, Z., Zou, H., Shao, L., Sun, Laixiang, Dong, G., Fan, D., Huang, X., Frost, L.,
800 Fox-James, L. 2019. An index-based assessment of perceived climate risk and vulnerability for
801 the urban cluster in the Yangtze River Delta Region of China. *Sustainability* 11, 2099,
802 doi:10.3390/su11072099.
- 803 Teng, J., Jakeman, A. J., Vaze, J., et al. 2017. Flood inundation modelling: A review of methods,
804 recent advances and uncertainty analysis. *Environmental Modelling & Software*, 90: 201-216.
- 805 Thomson, A.M., Calvin, K.V., Smith, S.J. et al. 2011. RCP4.5: A pathway for stabilization of radiative
806 forcing by 2100. *Climatic Change*, 109: 77-94. <https://doi.org/10.1007/s10584-011-0151-4>.
- 807 United Nations, Department of Economic and Social Affairs, Population Division. 2018. *The World's*
808 *Cities in 2018 – Data Booklet (ST/ESA/SER.A/417)*.
- 809 USGCRP (U.S. Global Change Research Program). 2014. *National Climate Assessment, Chapter 26:*
810 *Decision Support.* Available at: <https://nca2014.globalchange.gov/downloads>.
- 811 Voorberg, W. H., Bekkers, V. J., Tummers, L. G. 2015. A systematic review of co-creation and
812 co-production: Embarking on the social innovation journey. *Public Management Review*, 17(9),

- 813 1333-1357.
- 814 Wang, J., Yi, S., Li, M., Wang, L., Song, C. 2018. Effects of sea level rise, land subsidence,
815 bathymetric change and typhoon tracks on storm flooding in the coastal areas of Shanghai.
816 *Science of the Total Environment* 621, 228–234.
- 817 Wang, X., Yin, Z-E., Chi, X.-X., Yin, J. 2015. Characteristics of different magnitude precipitation
818 change in Shanghai during 1961—2010. *J. Earth Env.* 6(3), 161-167. (In Chinese)
- 819 Wang, Y. Y. 2001. Technical Report: Flood damage assessment in Shanghai city. Flood risk map of
820 Shanghai. IWRH. Beijing. (in Chinese)
- 821 Westra, S., Alexander, L. V., Zwiers, F. W. 2013. Global increasing trends in annual maximum daily
822 precipitation, *J. Clim.*, 26, 3904–3918.
- 823 Westra, S., Fowler, H. J., Evans, J. P., Alexander, L. V., Berg, P., Johnson, F., Kendon, E. J., Lenderink,
824 G., Roberts, N. M. 2014. Future changes to the intensity and frequency of short duration extreme
825 rainfall, *Rev. Geophys.*, 52, 522–555, doi:10.1002/2014RG000464.
- 826 Wu, P., Christidis, N., Stott P. 2013. Anthropogenic impact on Earth’s hydrological cycle. *Nature*
827 *Climate Change*. 3: 807-810.
- 828 Wu, J., Yang, R., Song, J. 2018. Effectiveness of low-impact development for urban inundation risk
829 mitigation. *Natural Hazards and Earth System Sciences* 18, 2525–2536.
830 <https://doi.org/10.5194/nhess-18-2525-2018>.
- 831 Wu, W., Mu, H., Liang, Z., et al. 2016. Projected changes in extreme temperature and precipitation
832 events in Shanghai based on CMIP5 simulations. *Climatic and Environmental Research* (in
833 Chinese), 21(3), 269-281, doi: 10.3878/j.issn.1006-9585.2016.14225.
- 834 Yuan, Y., Xu, Y.-S., Arulrajah, A. 2017. Sustainable measures for mitigation of flooding hazards: A
835 case study in Shanghai, China. *Water* 9, 310, 1-16. doi:10.3390/w9050310.

Table 1. Cost analysis of the five individual solutions

Solutions	Initial Cost (million RMB)	Unit (km/km ²)	Maintenance and operations	Life span (year)	Life cycle cost (million RMB)	Salvage Value (Million RMB)	Annual Average Cost (million RMB/y)
Drainage	100/km	117.6	2%	50	13,427	52	269
Green	600/km ²	30.0	2%	70	17,988	36	257
Tun30	300/km	22.2	5%	50	14,070	29	281
Tun50	300/km	37.0	5%	50	23,451	49	469
Tun70	300/km	51.8	5%	50	32,831	68	657

Note: Drainage: drainage capacity enhancement; Green: green area increase; Tun30, Tun50, Tun70: deep tunnel with 30%, 50%, 70% runoff absorbed, respectively.

Table 2. Cost-effectiveness of the solutions

	ARR (Average risk reduction rate, %)	PVC (million RMB/year)	ARR/PVC (percentage point/million RMB/year)
Drainage	25	269	0.093
Green area	26	257	0.101
Tun30	39	281	0.139
D+G	62	526	0.118
Tun50	74	469	0.158
D+G+Tun30	85	807	0.105
Tun70	87	657	0.132

Note: ARR: Average risk reduction rate. PVC: The present value of cost per year.

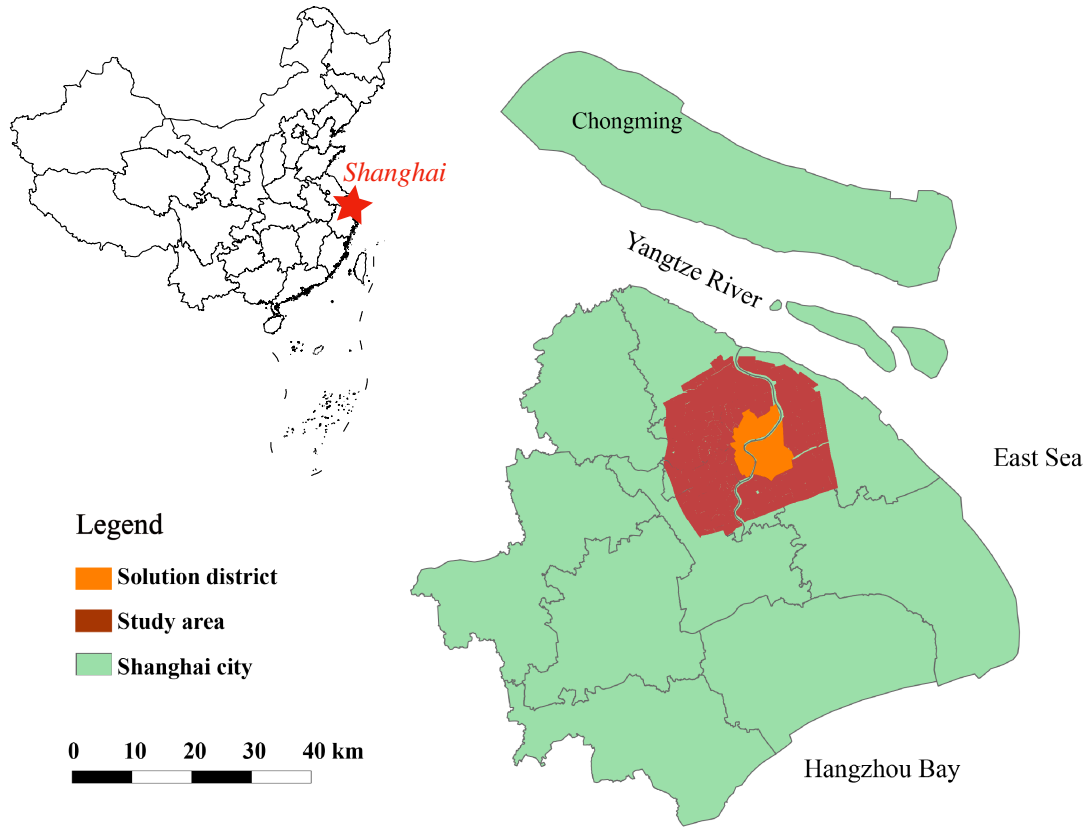


Fig.1 Shanghai and the study area

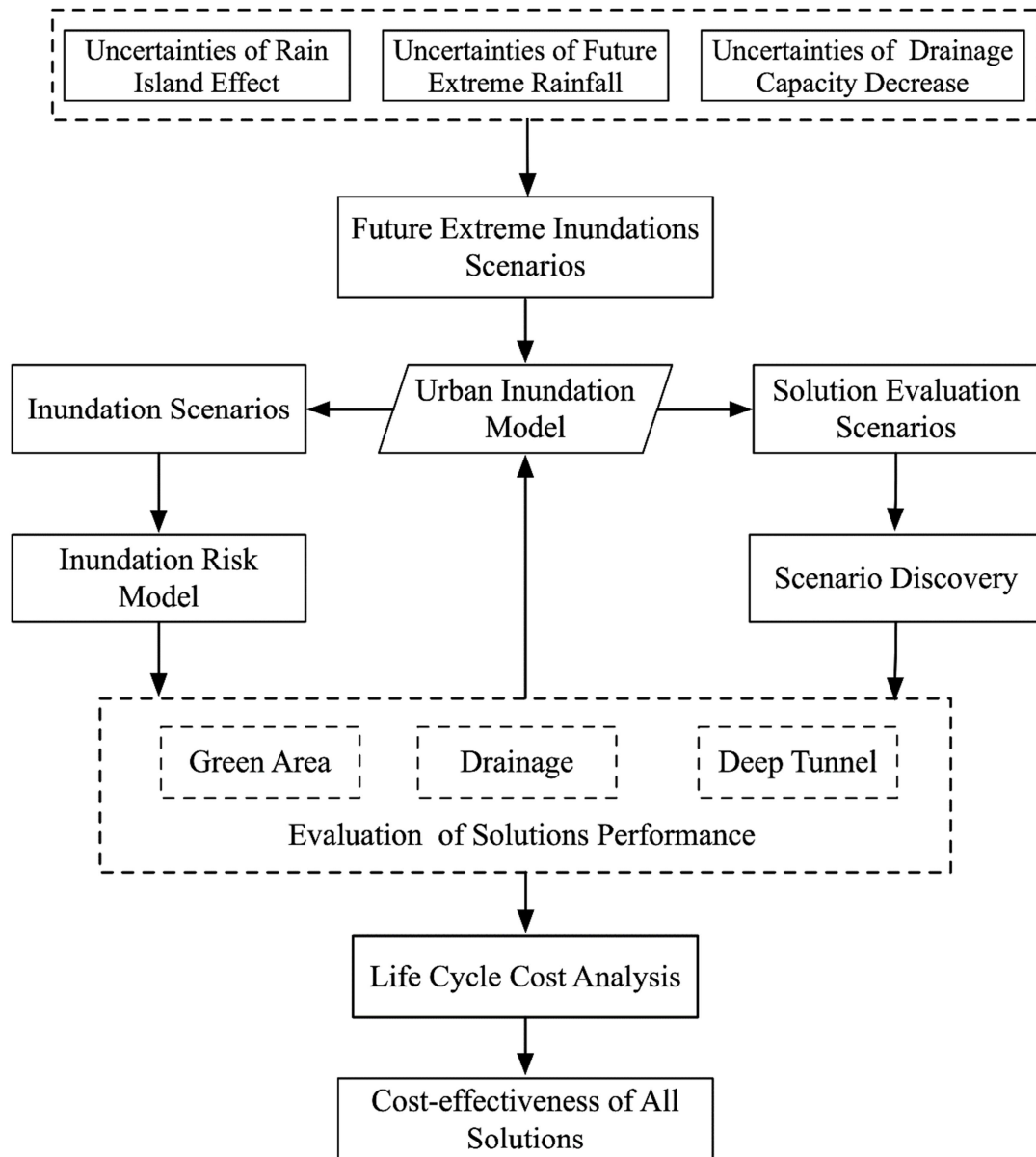


Fig. 2 Coupling flood model, risk model and evaluation model in many plausible scenarios: flow chart.

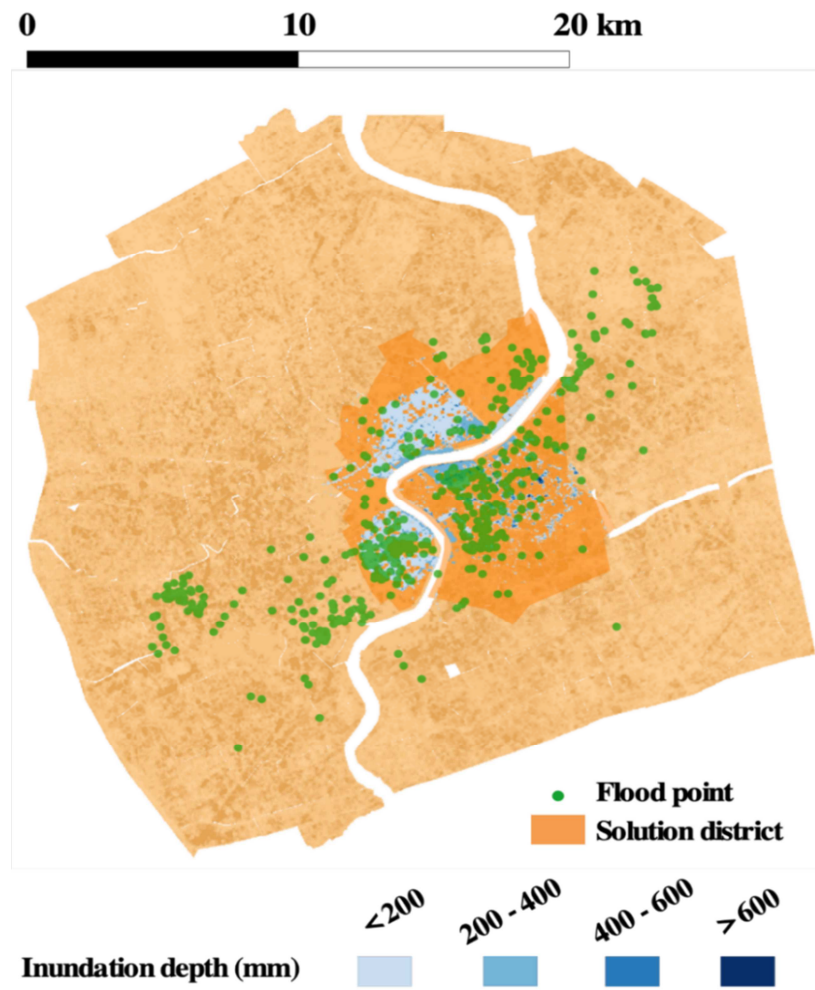


Fig. 3 Validation of Shanghai UIM simulation using public-reported waterlogging points

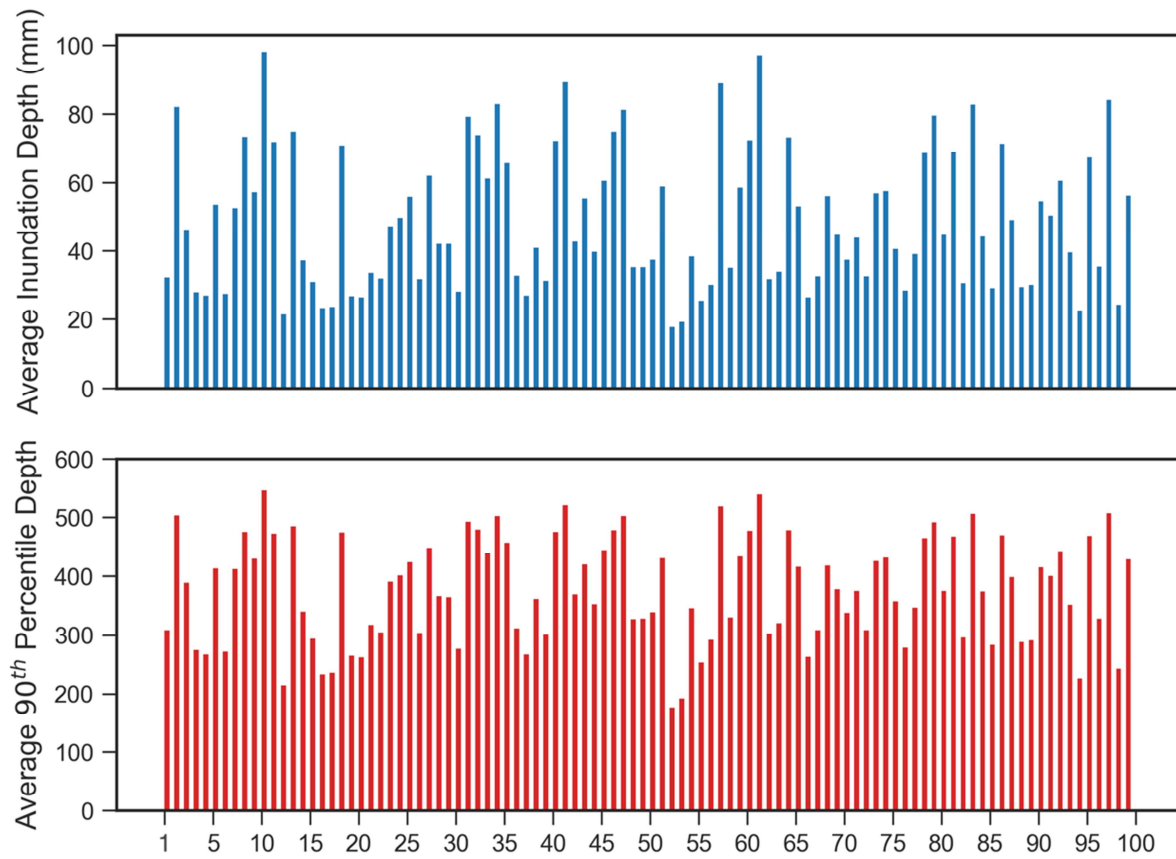


Fig. 4. Average inundation depth (upper figure) and average 90th percentile depth (lower figure) in the 100 inundation scenarios (scenario ID number on the x-axis)

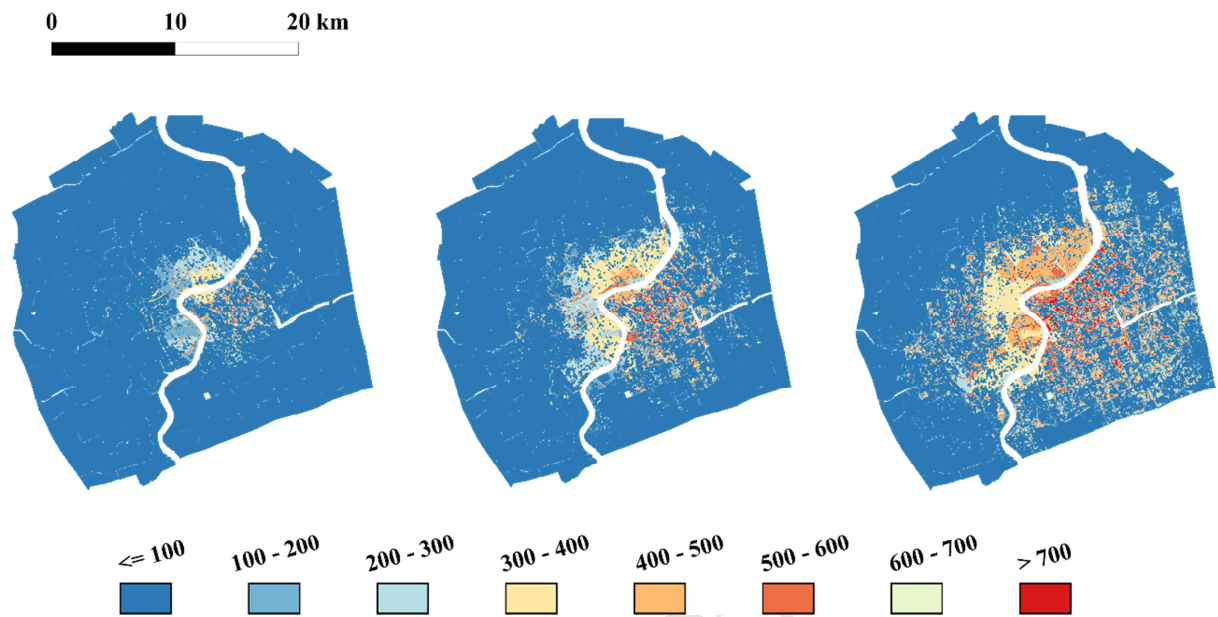


Fig. 5. Comparison of Inundation area and depth (mm): Sc-53 (left), Sc-3 (middle), Sc-11 (right). The α , β_1 and γ values of these three scenarios are presented in Table S2 of SM. The corresponding damage/loss maps are presented in Figure S1 of SM.

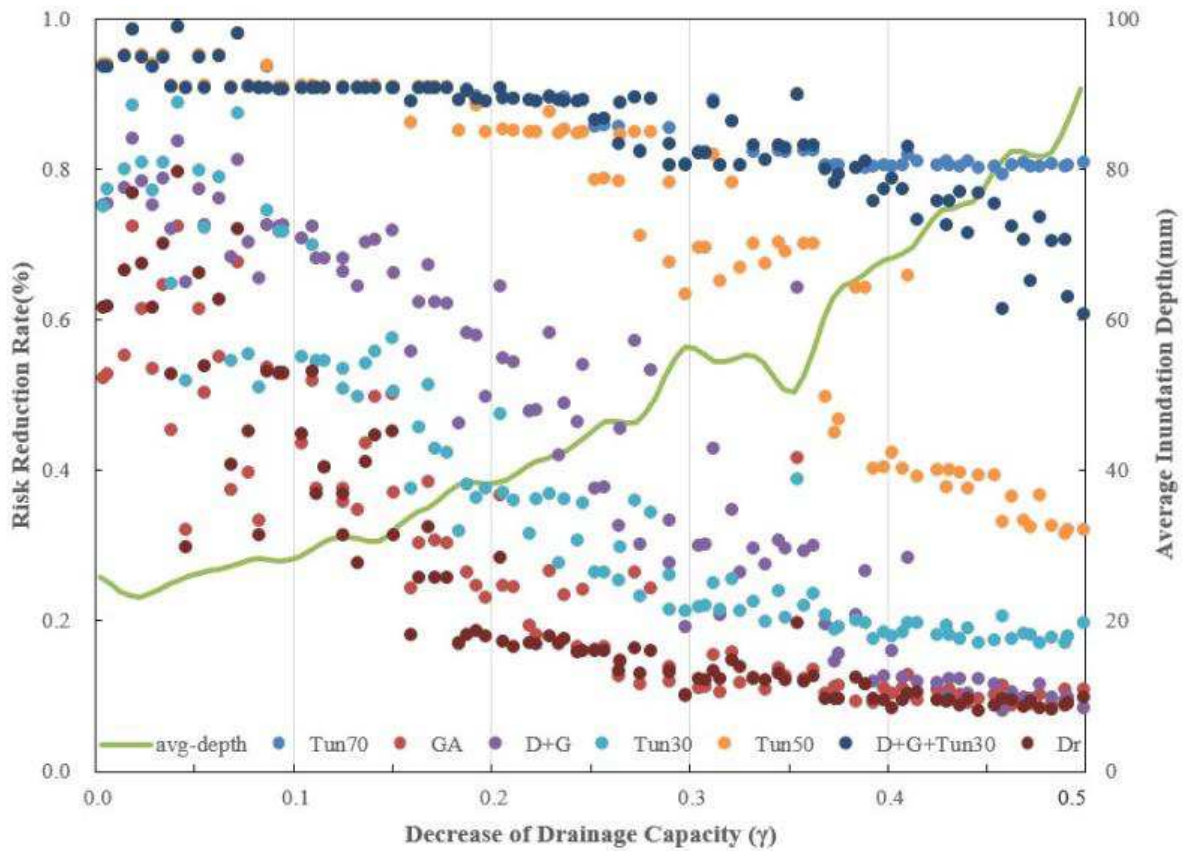


Fig. 6. Risk reduction rate of the seven selected strategies and the average inundation depth across the combinations of solution and rainfall scenarios at the given level of γ . Tun70: deep tunnel with 70% runoff absorbed under the baseline; GA: green area expansion; D+G: drainage enhancement + GA; Tun30: deep tunnel with 30% runoff absorbed under the baseline; D+G+Tun30: drainage enhancement + green area + Tun30; Tun50: deep tunnel with 50% runoff absorbed under the baseline; Dr: drainage enhancement.

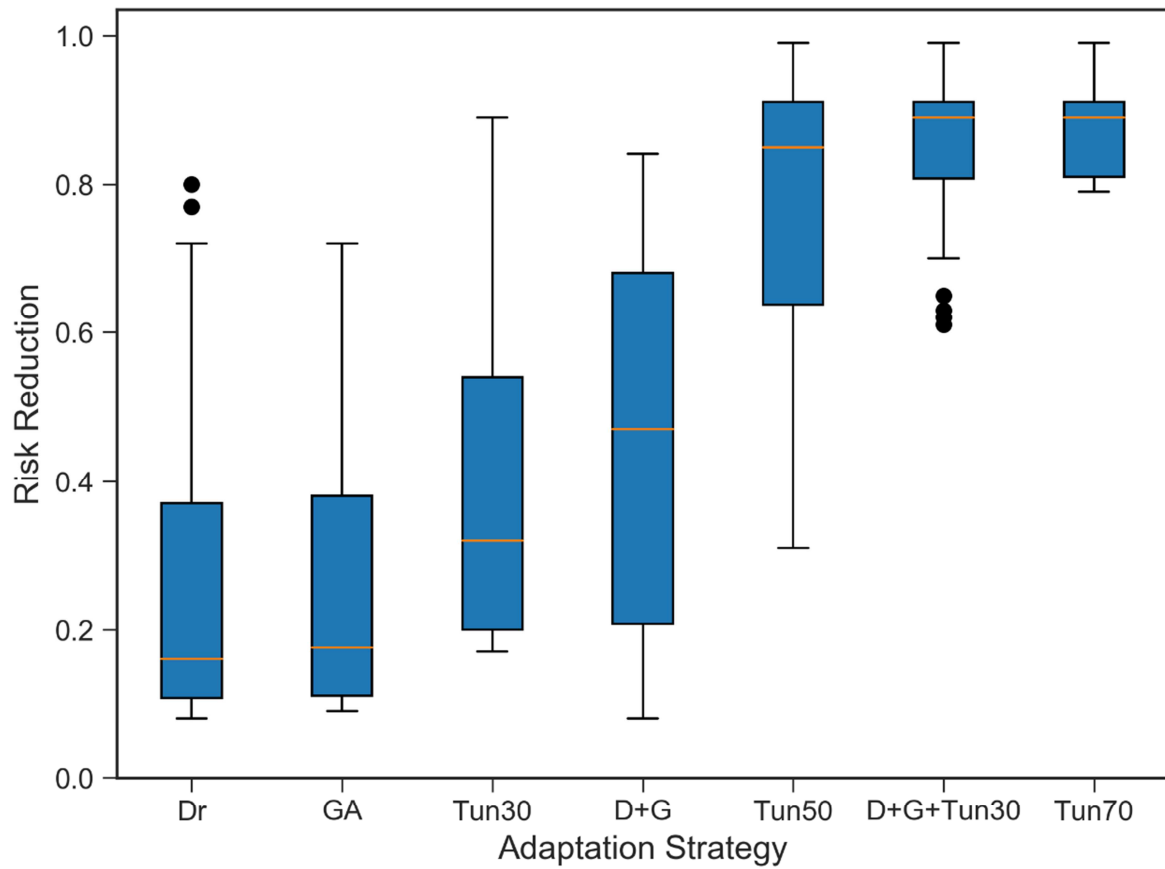


Fig. 7. Box plots of potential risk reduction rates. Dr: drainage capacity enhancement; GA: green area increase; Tun30: deep tunnel with 30% runoff absorbed; D+G: Dr + GA; Tun50: deep tunnel with 50% runoff absorbed; D+G+Tun30: Dr + GA + Tun30; Tun70: deep tunnel with 70% runoff absorbed

Synthesized trade-off analysis of flood control solutions under future deep uncertainty: An application to the central business district of Shanghai

Highlights

- Flexible testing of multiple flood control solutions under the condition of deep uncertainties
- Reoccurrence in the 2050s of a record-breaking extreme rainfall event in central Shanghai
- Sea-level rise and land subsidence will be the key concern of flood control in the future
- A combination of grey and green infrastructures is the preferred solution
- A successful synthesized trade-off analysis is bound to be a knowledge co-creation process

Declaration of interests

The authors declare that they have no known competing financial interests or personal relationships that could have appeared to influence the work reported in this paper.

The authors declare the following financial interests/personal relationships which may be considered as potential competing interests:



Laixiang Sun (and on behalf of all coauthors)

Corresponding Author

LSun123@umd.edu, Tel: +1-301-405-8131, Fax: +1-301-314-9299